



CHORUS

This is the accepted manuscript made available via CHORUS. The article has been published as:

Doping SrTiO₃ supported FeSe by excess atoms and oxygen vacancies

K. V. Shanavas and David J. Singh

Phys. Rev. B **92**, 035144 — Published 24 July 2015

DOI: [10.1103/PhysRevB.92.035144](https://doi.org/10.1103/PhysRevB.92.035144)

Doping SrTiO₃ supported FeSe by excess atoms and oxygen vacancies

K. V. Shanavas* and David J. Singh

Materials Science and Technology Division, Oak Ridge National Laboratory, Oak Ridge, Tennessee 37831-6056, USA

(Dated: July 7, 2015)

Photoemission studies of FeSe monolayer films on SrTiO₃ substrate have shown electronic structures that deviate from pristine FeSe, consistent with heavy electron doping. With the help of first-principles calculations we studied the effect of excess Fe and Se atoms on the monolayer and oxygen vacancies in the substrate in order to understand the reported Fermi surface in this system. We find that both excess Fe and Se atoms prefer the same adsorption site above the bottom Se atoms on the monolayer. The adsorbed Fe is strongly magnetic and contributes electrons to the monolayer, while excess Se hybridize with the monolayer Fe-*d* states and partially opens a gap just above the Fermi energy. We also find that the 2D electron gas generated by the oxygen vacancies is partly transferred to the monolayer and can potentially suppress the hole pockets around the Γ point. Thus, both O vacancies in the SrTiO₃ substrate and excess Fe over the monolayer can provide high levels of electron doping.

I. INTRODUCTION

Superconductivity in Fe-based materials is particularly interesting in part because of its interplay with magnetism¹⁻⁵ and simple systems such as FeSe and FeSe_{1-x}Te_x have attracted significant attention in recent years.^{6,7} The bulk form of FeSe has a superconducting transition temperature (T_c) of 8 K, which can be enhanced upto 37 K with pressure.⁷⁻⁹ Experimental measurements on single-layer FeSe films grown over SrTiO₃ (STO) substrate show that, the samples that are metallic at room temperatures open a gap of 15-20 meV when cooled, which has been attributed to a possible onset of superconductivity in this system.¹⁰⁻¹⁵ The transition is reported to be above $T_c = 65$ K, with gaps of 15-20 meV. Interestingly, the effect is not observed in double layers or more,¹⁶ in contrast to FeSe films on graphene where a transition at 2.2 K was reported on 30 nm thick samples.¹⁷ This has led to the speculation that the interface plays a crucial role in the properties of monolayer FeSe.¹⁸

Photoelectron spectroscopy measurements showed that, unlike other Fe based superconductors, the Fermi surface of single-layer FeSe on STO consists only electron pockets at the zone corners without the hole pockets around zone center.¹¹ This means that the sign-changing *s*-wave pairing state from spin fluctuation exchange in Fe based superconductors cannot exist here and points to a different mechanism of gap opening.⁵ Interestingly, measurements on samples with different annealing showed that as-prepared samples do have the hole pockets around Γ point, but remain metallic to low temperatures.¹⁹ Annealing in vacuum removes the hole pocket and also leads to the transition. Electron doping was suggested as a possible cause for the transition,¹⁹⁻²² which could arise from Se or O vacancies during the annealing process. However, theoretical studies showed that Se vacancies in this system lead to hole doping.²³ Scanning tunneling spectroscopy measurements on films grown on pure STO substrate find the as-prepared samples to be semiconducting and containing excess Se.²⁴ Oxygen vacancies have been known to induce highly mobile 2D electron gas at the

polar interfaces involving SrTiO₃.²⁵

Here, we study the effect of excess Fe and Se on the monolayer as well as oxygen vacancies in the substrate, in order to understand the observed Fermi surface of 1uc-FeSe on STO. We find that the excess atoms prefer a site directly above the bottom Se atoms in the FeSe monolayer similar to excess Fe in bulk FeTe and that the excess Fe contributes electrons to the monolayer Fe-*d* states that may suppress the hole pockets observed around Γ point. Excess Se, on the other hand, contributes *p*-states that hybridize strongly with the monolayer Fe and lead to significant changes in the band dispersion around Fermi level. It also suppresses the hole pockets, but at the same time shrinking the electron pockets and inducing a pseudogap just above the Fermi level. The 2D electron gas (2DEG) formed at the STO surface due to oxygen vacancies can lead to an effective attraction between STO and FeSe, also leading to electron doping in the monolayer.

II. METHODS

To study the monolayer FeSe on SrTiO₃ (001) surface, we used a symmetric TiO₂ terminated slab, 5.5 unitcell long along *c* axis separated by a vacuum layer of ~ 20 Å. To accommodate the striped antiferromagnetic structure, the unitcell is enlarged to be $\sqrt{2}a \times \sqrt{2}a$ parallel to the surface. The FeSe monolayers are then added to both top and bottom surfaces of the slab to preserve symmetry and half of this unitcell is shown in Fig. 1. The structure is then optimized with spin-polarization, allowing the *z* coordinates of the atoms to vary. The necessity of including magnetism in standard density functional structure optimizations of Fe-based superconductors is well established and has been associated with the unusual magnetic character of these compounds.³ We tested the convergence of structural parameters with a 7.5 unitcell STO slab and found them to be similar.

In our calculations we consider 25% doping with excess atoms, that correspond to FeSeX_{0.25} where X=Fe,Se. As shown in Fig. 1, there are three sites where the excess

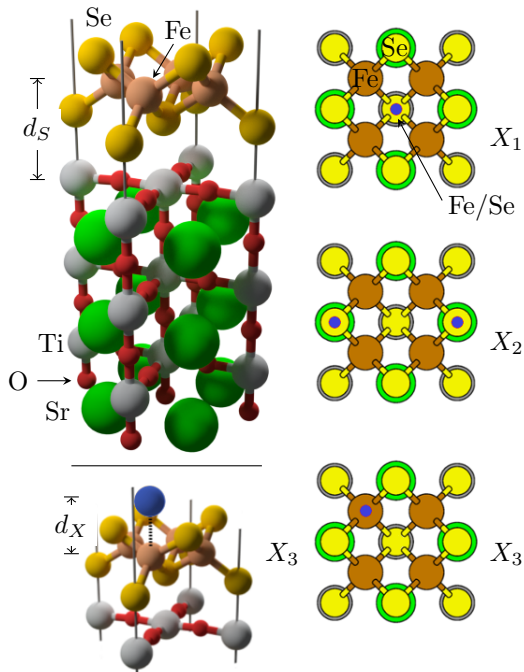


FIG. 1. Half the unitcell of monolayer FeSe on SrTiO₃ used in the calculations is shown on the left. On the right, the top views of the unitcell is shown indicating the three binding sites for excess Fe/Se atoms by blue dots. The side view of the X₃ configuration is shown bottom left. The distances are defined as $d_S = z_{\text{Ti}} - z_{\text{Fe}}$ and $d_X = z_X - z_{\text{Fe}}$, where z_i are the z coordinate of the atom i .

atoms can potentially bind with FeSe. The site X₁ corresponds to one directly above the bottom Se atom of the monolayer as indicated by the blue dot. The site X₂ lies above to one of the two Se atoms on the top of the FeSe monolayer, while X₃ correspond to a site above Fe. The surface to monolayer distance is measured as the distance along z axis between Fe and Ti ions, $d_S = z_{\text{Fe}} - z_{\text{Ti}}$ and the monolayer to excess atom distance is defined as, $d_X = z_X - z_{\text{Fe}}$. Finally, to simulate the 2DEG at the STO surface that arise because of oxygen vacancies we replace oxygen atoms at the STO surface partially by F using virtual crystal approximation (VCA). Since F atoms have one more electron than O, replacing the latter with O_{1-x}F_x leads to $2x$ electrons per surface unitcell. These electrons are confined close to the surface along z , but have large dispersion in the in-plane directions.

All electronic structure calculations are carried out within the density functional theory as implemented in VASP code,²⁶ using projector augmented waves²⁷ and generalized gradient approximation²⁸ with Perdew-Burke-Ernzerhof parametrization. Kinetic energy cutoff for the plane wave basis is taken to be 450 eV and a $11 \times 11 \times 1$ Monkhorst-Pack grid is used for reciprocal space sampling. The vdW interaction is explicitly included in the calculation employing the method devel-

oped by Grimme,²⁹ to properly describe the attraction between the substrate and monolayers. Structural relaxations are carried out till forces are less than 0.02 eV/Å.

III. RESULTS

The in-plane lattice parameters of the supercell are set to 5.52 Å, the relaxed bulk lattice constant of SrTiO₃. Full ionic relaxations are then performed keeping the cell dimensions fixed and with the striped antiferromagnetic phase for Fe moments, which is the ground state for this system.³⁰ We find that including the vdW interaction leads an effective attraction between the surface and the monolayer and reduces the surface Ti to monolayer Fe distance (d_S from Fig. 1) from 4.44 Å to 4.19 Å, which corresponds to a Ti-Se distance of 2.91 Å. The final structure is then used to calculate the non-magnetic band structure and partial density of states (PDOS) shown in Fig. 2.

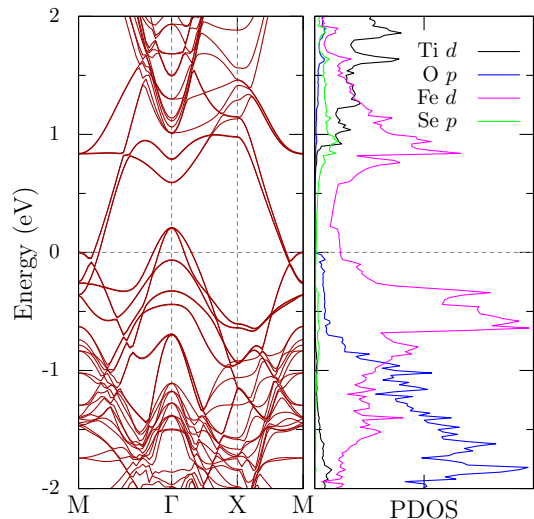


FIG. 2. The non-magnetic electronic band structure and partial density of states (PDOS) for optimized structure of STO+FeSe with van der Waal's interactions. The bands around Fermi level have strong Fe- d character and exhibit hole pockets around Γ and electron pockets around M points.

The valence states from the substrate have O- p character and lie below -0.8 eV, while the conduction states are above 1 eV and are made of Ti- t_{2g} as can be seen from the PDOS in Fig. 2. Thus, the Fermi energy of the composite STO+FeSe system lie around midway in the substrate band gap and the electronic structure around the Fermi energy is from the FeSe. The Fe- d bands cross the Fermi level and form hole pockets around the Γ point and electron pockets around M points, similar to bulk FeSe.³¹

The electronic density of states at the Fermi level is $N(E_F) = 1.24 \text{ eV}^{-1}$ per Fe atom and is distributed be-

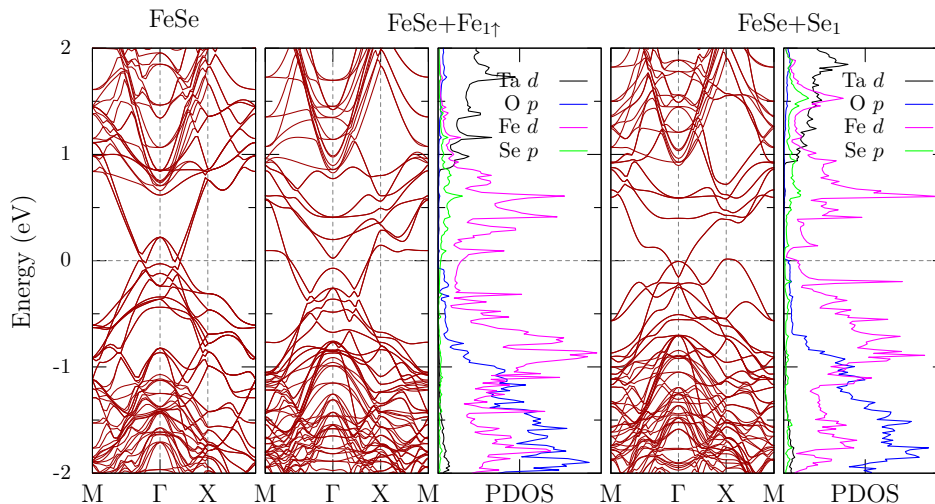


FIG. 3. Non-spin-polarized band structures and density of states in the doubled unit cell of STO+FeSe bare, with excess Fe and with excess Se in the lowest energy configurations. The doubling of the unitcell folds the electron and hole pockets to the zone center. The excess Fe is treated as magnetic.

tween the electron and hole states. In Fig. 2, we can clearly see the step-like features in Fe- d partial DOS that indicate the two-dimensional character of the band structure. From the spin-polarized calculation we get a magnetic moment of $2.4 \mu_B$ per Fe. The Se- p states lie between -3 and -5 eV and exhibit strong covalent coupling with Fe- d orbitals.

A. Excess Fe and Se on FeSe

Next, excess Fe and Se atoms are added at the sites shown in Fig. 1 and the structures are fully relaxed within the striped antiferromagnetic order in separate calculations. Results are summarized in Table I. Surprisingly, the same site X_1 is found to have the lowest energy for both excess anion and cation adsorption. This site is neither a good cation site nor a good anion site, but rather favors more covalent bonding, as was previously noted in the case of FeTe. This leads to the unusual monovalent state of excess Fe.³² This site also allows closest distances between excess atoms and the monolayer with $d_X = 1.51 \text{ \AA}$ and 1.60 \AA for Fe and Se respectively. As can be seen from the table, the magnetic moments of the iron atoms in the monolayer diminish from the bare values upon doping. The reduction is larger for Se doping; in the case of Se₁, the average Fe moments are $1.82 \mu_B$ reduced from $2.38 \mu_B$. The excess Fe is found to be strongly magnetic, with moments of 2.8, 3.1 and $2.6 \mu_B$ for Fe₁, Fe₂ and Fe₃ respectively, consistent with excess Fe calculations on bulk FeTe.³²

Consistent with previous calculations,²³ we find that Se doping removes of the electrons from the Fe- d orbitals, evidence for which can be seen from the partial density of states plots in Fig. 3. The partial Fe- d DOS for the

TABLE I. Calculated energy differences, atomic distances and magnetic moments of the layer Fe atoms for the STO+FeSe system with excess Fe and Se atoms. The structures are optimized in the striped antiferromagnetic phase.

	bare	Fe ₁	Fe ₂	Fe ₃	Se ₁	Se ₂	Se ₃
$E - E_0$ (eV/f.u.)	-	0.00	0.71	0.42	0.00	0.17	0.28
d_S (Å)	4.19	4.28	4.22	4.29	4.29	4.25	4.15
d_X (Å)	-	1.51	3.43	2.55	1.60	3.62	2.87
m_{Fe} (μ_B)	2.38	2.26	2.11	2.30	1.82	2.09	1.29

FeSe+Se₁ is shifted upward compared to the same plot in Fig. 2. As a consequence, the Fe moments are reduced substantially as shown in Table I upon Se doping. On the other hand Fe₁ donates electrons to the monolayer, shifting the Fe- d bands lower. For the Fe doped electronic structure plots in Fig. 3, the excess Fe is allowed to be spin-polarized while keeping the monolayer atoms close non-magnetic. This was done to keep the correct number of electrons in the monolayer.

Dispersion of the layer Fe bands is modified by the presence of excess atoms on the monolayer. In the case of Fe₁, the Fe- d bands are shifted downward, which removes the hole pockets and makes the electron pockets deeper as shown in Fig. 2. The effect of excess Se is more pronounced; overlap of Se- p orbitals with Fe- d changes the shape of electron and hole pockets. A new hole pocket appears around the X point in the new Brillouin zone while the electron pocket around Γ (around M in the smaller unitcell) shrinks in size. Also, the density of states drops to almost zero, opening a pseudogap of ~ 0.15 eV just above the Fermi level in the Se doped case.

The effect of excess atoms on the monolayer Fe DOS is shown in Fig. 4. In the case of excess Fe, the Fe₁- d states lie -2 eV below the Fermi level and shifts the monolayer

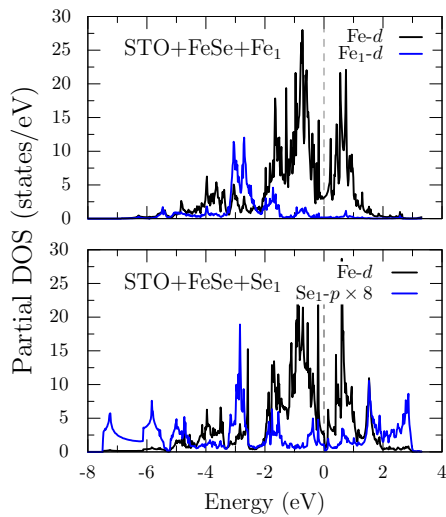


FIG. 4. Partial density of states of states of the monolayer Fe- d and the excess Fe $_1$ - d (top) and the excess Se $_1$ - p (bottom). Fermi level is set to zero.

Fe- d states to lower energies via electron doping. The Se $_1$ - p states, on the other hand, have large dispersion and overlap with Fe- d across a wide range. This leads to rearrangement of the Fe- d states and the observed depletion of density just above the Fermi level.

B. Oxygen vacancies in STO

Bare SrTiO $_3$ surfaces with TiO $_2$ termination are known to develop a 2D electron gas which is localized to within few unitcells. It is believed to originate from oxygen vacancies at the surface, that leave two electrons per vacancy in the Ti- t_{2g} orbitals. It is to be expected that some of this charge will be transferred to the FeSe, affecting the Fermi surface of the monolayer, although the amount is unclear a priori. To test this, we calculated the electronic structure of STO+FeSe with a 2DEG on the STO substrate.

In order to generate a 2DEG on SrTiO $_3$ without reducing symmetry, we replaced 20% of the surface oxygen atoms with fluorine using virtual crystal approximation (VCA). This leads to 0.4 electrons per surface unitcell (there are two O per surface cell for TiO $_2$ termination) which corresponds to an electron density, $n_e \sim 10^{20}$ cm $^{-2}$ on the surface. Note that, actual 2DEG densities at the experimental conditions will depend on the number of oxygen vacancies and other defects generated during the surface preparation and the FeSe deposition. As expected, these additional electrons reside in the Ti t_{2g} bands near the surface as shown in Fig. 5(a).

Next, using the relaxed structure with vdW interactions (with $d_S = 4.19$ Å), we calculated the band structure with surface 2DEG, which is plotted in Fig. 5(b). Compared to Fig. 2, we find that the FeSe bands have

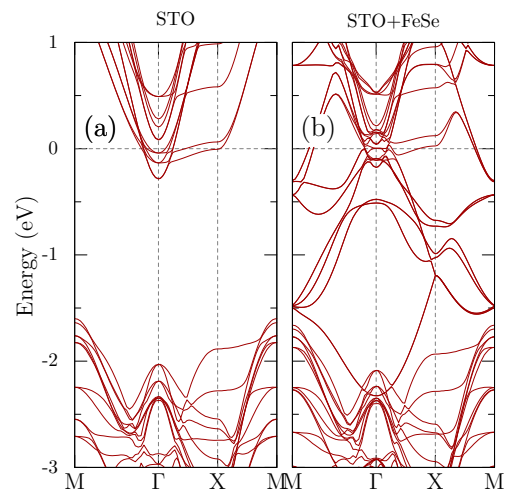


FIG. 5. (Color online) (a) Electronic structure of bare SrTi(O $_{1-x}$ F $_x$) $_3$ slab calculated within virtual crystal approximation with $x = 0.2$, to simulate 2DEG at the surface. (b) Band structure of STO and FeSe monolayer system in the presence 2DEG on STO.

shifted up by about 1 eV. Closely inspecting the bands around the Fermi level, we can see evidence of charge transfer from STO to the monolayer. Counting the states gives about 0.1 extra electrons per Fe, reducing the surface 2DEG to 0.21 electrons. However, hole pockets around Γ are not fully removed since the pockets are 0.11 holes per Fe deep and secondly some of the transferred charge goes to the electron pocket around M. From the relative change in size of the two pockets we estimate that 0.07 electrons go to the hole pocket, which is not sufficient to fully remove it. Two scenarios that can potentially increase the electron doping of FeSe monolayer are a) higher 2DEG density at the STO which can transfer more charge to the monolayer and b) reduced substrate to monolayer distance due other interactions arising from other sources.

We estimated the effect of distance between STO and monolayer on the charge transfer and the results are summarized in Fig. 6. We find that, the charge transferred from the 2DEG to FeSe increases as the distance is reduced. Below a distance $d_S = 3.8$ Å, the hole states around the Γ in the FeSe band structure is completely suppressed, while the electron pocket around M remains more or less unaffected. However, this requires an additional displacement of 0.4 Å of the monolayer towards the surface from the relaxed distance of $d_S = 4.19$ Å obtained in the previous section. The electrostatic attraction resulting from the charge transfer can potentially reduce d_S further and analyzing the forces on the atoms we estimate this reduction to be about 0.1 Å.

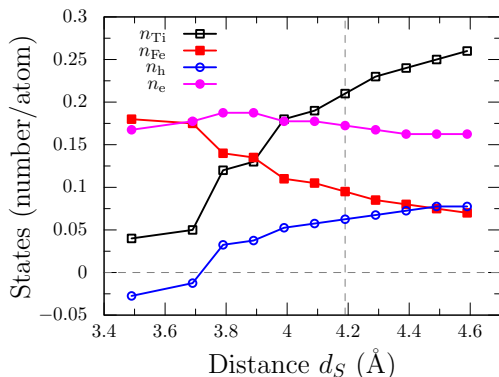


FIG. 6. (Color online) Charge transfer from STO to FeSe as a function of distance between the two. n_{Ti} and n_{Fe} are the additional electrons in Ti- t_{2g} and Fe- d states from VCA calculations and $n_{Ti} + 2n_{Fe} = 0.4$. n_e and n_h are the number of electrons and in the pockets around M and Γ point respectively. The vertical dashed line correspond to the vdW relaxed distance without charges. The hole states are completely removed below 3.8\AA .

IV. CONCLUSIONS

We studied the effect of excess atoms and oxygen vacancies on the electronic structure of $\text{SrTiO}_3 + \text{FeSe}$ system with the help of first principles calculations. We find that the vdW interactions play an important role in stabilizing the system. The excess atoms prefer the X_1 site above the lower Se atoms that allows them to bond strongly to the surface. The excess Fe atoms are magnetic while the Se atoms bond strongly with the layer Fe. The oxygen vacancies induce a 2DEG on the SrTiO_3 surface which is partially transferred to the monolayer. Thus, we identify two mechanisms for electron doping of FeSe monolayers on SrTiO_3 : (1) O deficiency at the SrTiO_3 surface and (2) excess Fe. While excess Fe and Se defects are mutually exclusive, a reducing environment favors both excess Se and oxygen vacancies.

V. ACKNOWLEDGMENTS

This research was supported by the US Department of Energy, Basic Energy Sciences, Office of Science, Materials Sciences and Engineering Division.

* kavungalvees@ornl.gov

- ¹ Yoichi Kamihara, Takumi Watanabe, Masahiro Hirano, and Hideo Hosono, "Iron-based layered superconductor $\text{La}[\text{O}_{1-x}\text{F}_x]\text{FeAs}$ ($x = 0.05 - 0.12$) with $T_c = 26$ K," *J. Am. Chem. Soc.* **130**, 3296 (2008).
- ² Clarina de la Cruz, Q. Huang, J. W. Lynn, Jiyang Li, W. Ratchiff II, J. L. Zarestky, H. A. Mook, G. F. Chen, J. L. Luo, N. L. Wang, and P. Dai, "Magnetic order close to superconductivity in the iron-based layered $\text{LaO}_{1-x}\text{F}_x\text{FeAs}$ systems," *Nature* **453**, 899 (2008).
- ³ I. I. Mazin, D. J. Singh, M. D. Johannes, and M. H. Du, "Unconventional superconductivity with a sign reversal in the order parameter of $\text{LaFeAsO}_{1-x}\text{F}_x$," *Phys. Rev. Lett.* **101**, 057003 (2008).
- ⁴ David C. Johnston, "The puzzle of high temperature superconductivity in layered iron pnictides and chalcogenides," *Adv. Phys.* **59**, 803 (2010).
- ⁵ David Joseph Singh, "Superconductivity and magnetism in 11-structure iron chalcogenides in relation to the iron pnictides," *Sci. Technol. Adv. Mater.* **13**, 054304 (2012).
- ⁶ M. H. Fang, H. M. Pham, B. Qian, T. J. Liu, E. K. Vehstedt, Y. Liu, L. Spinu, and Z. Q. Mao, "Superconductivity close to magnetic instability in $\text{Fe}(\text{Se}_{1-x}\text{Te}_x)_{0.82}$," *Phys. Rev. B* **78**, 224503 (2008).
- ⁷ F.-C. Hsu, J.-Y. Luo, K.-W. Yeh, T.-K. Chen, T.-W. Huang, P. M. Wu, Y.-C. Lee, Y.-L. Huang, Y.-Y. Chu, D.-C. Yan, and M.-K. Wu, "Superconductivity in the PbO-type structure $\alpha\text{-FeSe}$," *Proc. Natl. Acad. Sci. U.S.A.* **105**, 14262 (2008).
- ⁸ Yoshikazu Mizuguchi, Fumiaki Tomioka, Shunsuke Tsuda, Takahide Yamaguchi, and Yoshihiko Takano, "Superconductivity at 27 K in tetragonal FeSe under high pressure," *Appl. Phys. Lett.* **93**, 152505 (2008).

- ⁹ S. Medvedev, T. M. McQueen, I. A. Troyan, T. Palasyuk, M. I. Eremets, R. J. Cava, S. Naghavi, F. Casper, V. Ksenofontov, G. Wortmann, and C. Felser, "Electronic and magnetic phase diagram of $\beta\text{-Fe}_{1.01}\text{Se}$ with superconductivity at 36.7 K under pressure," *Nat. Mater.* **8**, 630 (2009).
- ¹⁰ Wang Qing-Yan, Li Zhi, Zhang Wen-Hao, Zhang Zuo-Cheng, Zhang Jin-Song, Li Wei, Ding Hao, Ou Yun-Bo, Deng Peng, Chang Kai, Wen Jing, Song Can-Li, He Ke, Jia Jin-Feng, Ji Shuai-Hua, Wang Ya-Yu, Wang Li-Li, Chen Xi, Ma Xu-Cun, and Xue Qi-Kun, "Interface-induced high-temperature superconductivity in single unit-cell FeSe films on SrTiO_3 ," *Chinese Phys. Lett.* **29**, 037402 (2012).
- ¹¹ Defa Liu, Wenhao Zhang, Daixiang Mou, Junfeng He, Yun-Bo Ou, Qing-Yan Wang, Zhi Li, Lili Wang, Lin Zhao, Shaolong He, Yingying Peng, Xu Liu, Chaoyu Chen, Li Yu, Guodong Liu, Xiaoli Dong, Jun Zhang, Chuangtian Chen, Zuyan Xu, Jiangping Hu, Xi Chen, Xucun Ma, Qikun Xue, and X. J. Zhou, "Electronic origin of high-temperature superconductivity in single-layer FeSe superconductor," *Nature Commun.* **3**, 931 (2012).
- ¹² Shaolong He, Junfeng He, Wenhao Zhang, Lin Zhao, Defa Liu, Xu Liu, Daixiang Mou, Yun-Bo Ou, Qing-Yan Wang, Zhi Li, Lili Wang, Yingying Peng, Yan Liu, Chaoyu Chen, Li Yu, Guodong Liu, Xiaoli Dong, Jun Zhang, Chuangtian Chen, Zuyan Xu, Xi Chen, Xucun Ma, Qikun Xue, and X. J. Zhou, "Phase diagram and electronic indication of high-temperature superconductivity at 65 K in single-layer FeSe films," *Nat. Mater.* **12**, 605 (2013).
- ¹³ Shiyong Tan, Yan Zhang, Miao Xia, Zirong Ye, Fei Chen, Xin Xie, Rui Peng, Difei Xu, Qin Fan, Haichao Xu, Juan Jiang, Tong Zhang, Xinchun Lai, Tao Xiang, Jiangping

- Hu, Binping Xie, and Donglai Feng, "Interface-induced superconductivity and strain-dependent spin density waves in FeSe/SrTiO₃ thin films," *Nat. Mater.* **12**, 634 (2013).
- ¹⁴ J. J. Lee, F. T. Schmitt, R. G. Moore, S. Johnston, Y.-T. Cui, W. Li, M. Yi, Z. K. Liu, M. Hashimoto, Y. Zhang, D. H. Lu, T. P. Devereaux, D.-H. Lee, and Z.-X. Shen, "Interfacial mode coupling as the origin of the enhancement of T_c in FeSe films on SrTiO₃," *Nature* **515**, 245248 (2014).
- ¹⁵ R. Peng, X. P. Shen, X. Xie, H. C. Xu, S. Y. Tan, M. Xia, T. Zhang, H. Y. Cao, X. G. Gong, J. P. Hu, B. P. Xie, and D. L. Feng, "Measurement of an enhanced superconducting phase and a pronounced anisotropy of the energy gap of a strained FeSe single layer in FeSe:Nb : SrTiO₃/KTaO₃ heterostructures using photoemission spectroscopy," *Phys. Rev. Lett.* **112**, 107001 (2014).
- ¹⁶ Xu Liu, Defa Liu, Wenhao Zhang, Junfeng He, Lin Zhao, Shaolong He, Daixiang Mou, Fangsen Li, Chenjia Tang, Zhi Li, Lili Wang, Yingying Peng, Yan Liu, Chaoyu Chen, Li Yu, Guodong Liu, Xiaoli Dong, Jun Zhang, Chuangtian Chen, Zuyan Xu, Xi Chen, Xucun Ma, Qikun Xue, and X. J. Zhou, "Dichotomy of the electronic structure and superconductivity between single-layer and double-layer FeSe/SrTiO₃ films," *Nature Commun.* **5**, 10.1038/ncomms6047.
- ¹⁷ Can-Li Song, Yi-Lin Wang, Ye-Ping Jiang, Zhi Li, Lili Wang, Ke He, Xi Chen, Xu-Cun Ma, and Qi-Kun Xue, "Molecular-beam epitaxy and robust superconductivity of stoichiometric FeSe crystalline films on bilayer graphene," *Phys. Rev. B* **84**, 020503 (2011).
- ¹⁸ Zhi Li, Jun-Ping Peng, Hui-Min Zhang, Wen-Hao Zhang, Hao Ding, Peng Deng, Kai Chang, Can-Li Song, Shuai-Hua Ji, Lili Wang, Ke He, Xi Chen, Qi-Kun Xue, and Xu-Cun Ma, "Molecular beam epitaxy growth and post-growth annealing of FeSe films on SrTiO₃: a scanning tunneling microscopy study," *J. Phys.: Condens. Matter* **26**, 265002 (2014).
- ¹⁹ Junfeng He, Xu Liu, Wenhao Zhang, Lin Zhao, Defa Liu, Shaolong He, Daixiang Mou, Fangsen Li, Chenjia Tang, Zhi Li, Lili Wang, Yingying Peng, Yan Liu, Chaoyu Chen, Li Yu, Guodong Liu, Xiaoli Dong, Jun Zhang, Chuangtian Chen, Zuyan Xu, Xi Chen, Xucun Ma, Qikun Xue, and X. J. Zhou, "Electronic evidence of an insulator-superconductor crossover in single-layer FeSe/SrTiO₃ films," *Proc. Natl. Acad. Sci. U.S.A.* **111**, 1850118506 (2014).
- ²⁰ Junhyeok Bang, Zhi Li, Y. Y. Sun, Amit Samanta, Y. Y. Zhang, Wenhao Zhang, Lili Wang, X. Chen, Xucun Ma, Q.-K. Xue, and S. B. Zhang, "Atomic and electronic structures of single-layer FeSe on SrTiO₃(001): The role of oxygen deficiency," *Phys. Rev. B* **87**, 220503 (2013).
- ²¹ Timur Bazhiron and Marvin L Cohen, "Effects of charge doping and constrained magnetization on the electronic structure of an FeSe monolayer," *J. Phys.: Condens. Matter* **25**, 105506 (2013).
- ²² Fawei Zheng, Zhigang Wang, Wei Kang, and Ping Zhang, "Antiferromagnetic fese monolayer on SrTiO₃: The charge doping and electric field effects," *Sci. Rep.* **3**, 2213 (2013).
- ²³ Tom Berlijn, Hai-Ping Cheng, P. J. Hirschfeld, and Wei Ku, "Doping effects of se vacancies in monolayer FeSe," *Phys. Rev. B* **89**, 020501 (2014).
- ²⁴ Wenhao Zhang, Zhi Li, Fangsen Li, Huimin Zhang, Junping Peng, Chenjia Tang, Qingyan Wang, Ke He, Xi Chen, Lili Wang, Xucun Ma, and Qi-Kun Xue, "Interface charge doping effects on superconductivity of single-unit-cell FeSe films on SrTiO₃ substrates," *Phys. Rev. B* **89**, 060506 (2014).
- ²⁵ James N. Eckstein, "Oxide interfaces: Watch out for the lack of oxygen," *Nat. Mater.* **6**, 473 (2007).
- ²⁶ G. Kresse and J. Hafner, "Ab-initio molecular dynamics for liquid metals," *Phys. Rev. B* **47**, 558 (1993); G. Kresse and J. Furthmüller, "Efficient iterative schemes for *ab initio* total-energy calculations using a plane-wave basis set," *ibid.* **54**, 11169 (1996).
- ²⁷ P. E. Blöchl, "Projector augmented-wave method," *Phys. Rev. B* **50**, 17953 (1994).
- ²⁸ John P. Perdew, Kieron Burke, and Matthias Ernzerhof, "Generalized gradient approximation made simple," *Phys. Rev. Lett.* **77**, 3865 (1996).
- ²⁹ Stefan Grimme, Jens Antony, Stephan Ehrlich, and Helge Krieg, "A consistent and accurate ab initio parametrization of density functional dispersion correction (DFT-D) for the 94 elements H-Pu," *J. Chem. Phys.* **132**, 154104 (2010); Stefan Grimme, Stephan Ehrlich, and Lars Goerigk, "Effect of the damping function in dispersion corrected density functional theory," *J. Comp. Chem.* **32**, 1456 (2011).
- ³⁰ Kai Liu, Zhong-Yi Lu, and Tao Xiang, "Atomic and electronic structures of fese monolayer and bilayer thin films on SrTiO₃ (001): First-principles study," *Phys. Rev. B* **85**, 235123 (2012).
- ³¹ Alaska Subedi, Lijun Zhang, D. J. Singh, and M. H. Du, "Density functional study of FeS, FeSe, and FeTe: Electronic structure, magnetism, phonons, and superconductivity," *Phys. Rev. B* **78**, 134514 (2008).
- ³² Lijun Zhang, D. J. Singh, and M. H. Du, "Density functional study of excess Fe in Fe_{1+x}Te: Magnetism and doping," *Phys. Rev. B* **79**, 012506 (2009).